Vietnam Journal of Science and Technology ***59*** *(5) (2021) 643-661*

doi:10.15625/2525-2518/59/5/15478

INVESTIGATING EFFECT OF SURFACE ROUGHNESS PATTERN ON DYNAMIC PERFORMANCE OF MEMS RESONATORS IN VARIOUS TYPES OF GASES AND GAS RAREFACTION

Lam Minh Thinh[1], Phan Minh Truong[2], Trinh Xuan Thang[1], Ngo Vo Ke Thanh[1], Le Quoc Cuong[3], Nguyen Chi Cuong[1, 2, *]

[1]Research Laboratories of Saigon High-Tech-Park, Lot I3, N2 street, Saigon Hi-Tech-Park, district 9, Ho Chi Minh city, Viet Nam

[2]Institute for Computational Science and Technology, Room 311(A&B), SBI building, Quang Trung Software City, Tan Chanh Hiep ward, district 12, Ho Chi Minh city, Viet Nam

[3]Department of Information and Communications, Ho Chi Minh City, Viet Nam, 59 Ly Tu Trong street, Ben Nghe ward, district 1, Ho Chi Minh city, Viet Nam

[*]Emails: *1.cuong.nguyenchi@shtplabs.org*

Received: 9 November 2021; Accepted for publication: 9 September 2021

Abstract. In ambient gas environment, the squeeze film damping (SFD) is a dominant damping source to reduce the quality factor (Q-factor) of micro-beam resonators. At a thin gap spacing, the surface roughness pattern effect becomes more strongly because a gas flow is more restricted by the surface roughness. The average modified molecular gas lubrication (MMGL) equation, which is modified with the pressure flow factors and the effective viscosity, is utilized to analyze the squeeze film damping (SFD) on micro-beam resonators considering the effect of surface roughness pattern in various types of the gas and gas rarefaction. Three types of roughness pattern (longitudinal, isotropic, and transverse roughness) are considered. The thermoelastic damping (TED) and support loss are involved to calculate the total Q-factor of micro-beam resonator. The effect of surface roughness pattern (film thickness ratio and Peklenik number) on Q-factors of micro-beam resonators is then discussed. It is found that the effect of roughness pattern becomes more considerably on Q-factor in lower gas rarefaction (higher pressure) and higher effective viscosity of the gas. While, the effect of roughness pattern is significantly reduced as the effective viscosity of the gas decreases in higher mode of resonator and higher gas rarefaction.

Keywords: Quality factor of MEMS resonator, squeeze film damping, surface roughness pattern, gas rarefaction, types of gases.

Classification numbers: 5.2.4, 5.4.3, 5.4.4.

1. INTRODUCTION

Micro vibrational structures (such as micro-beam, bridge, plate, membrane, etc.), which are the most important structures of micro-electro-mechanical system (MEMS) resonators, can be

used in many sensing applications (such as gas, temperature, relative humidity, pressure, etc.), and high precision actuations [1]. In MEMS resonators, the resonant frequency and the quality factor (Q-factor) are important dynamic characteristics of the mechanical resonator. High Q-factor is a key requirement for high resolution, frequency stability, and high sensitivity of MEMS resonators.

In MEMS resonators, there are many dominant damping sources (such as external gas damping and internal structural damping) affecting their dynamic performance. In ambient gas environment, the squeeze film damping (SFD) is a dominant external damping source to reduce Q-factor of MEMS resonators as a gas flow is resisted in a small gap spacing during their transverse motion. To lower the external SFD and improve the Q-factor, a lower ambient pressure (p) is introduced within the thin gap spacing (h_0), thus the effect of gas rarefaction becomes important [2]. Also, the effect of surface roughness [3] becomes an important factor to be discussed because of the large surface area and volume ratio under gas ambient conditions. To model the SFD, the conventional Reynolds equation [4] was derived using the conventional lubrication theory. Fukui and Kaneko [5] derived the modified Reynolds equation with Poiseuille flow rate (Q_P) to model the effect of gas rarefaction. Also, the surface roughness effect can be solved by (1) mixed average film thickness functions [6], (2) average flow factors [3,7-10] for all surface roughness pattern directions, and (3) using the fractal model [11] to generate functions for random surface roughness. To consider the surface roughness patterns, Patir and Cheng [12] first proposed the modified Reynolds equation using flow factors. Bhushan and Tonder [13,14] extended the flow factors to consider the slip flow. Flow factors could be conveniently used for the modified molecular gas lubrication (MMGL) equation to model the SFD considering various surface roughness patterns. Li *et al.* [3] and Li and Weng [7] proposed a flow factor analysis to modify the molecular gas lubrication (MMGL) equation for the effect of surface roughness pattern. Li [8] used pressure flow factors to modify the linearized MMGL equation including the coupled effects of roughness and gas rarefaction in MEMS devices.

Generally, the surface roughness pattern effect is characterized by the film thickness ratio (H_S) and the Peklenik number (γ). Also, the effect of gas rarefaction is represented by the inverse Knudsen number (D) and the accommodation coefficients, ACs (α). Flow factors [15, 16] are used to modify the MMGL equation to discuss the effects of gas rarefaction and surface roughness in MEMS devices. However, the effect of ACs has not been considered. Li [17] proposed a complete database of Poiseuille flow rates ($Q_P(D,\alpha_1,\alpha_2)$) in a wide range of gas rarefaction D ($0.01 \le D \le 100$) and ACs ($0.1 \le \alpha_1, \alpha_2 \le 1.0$) conditions. The effect of surface roughness on the dynamic coefficients of SFD in MEMS devices with symmetric ACs ($\alpha_1 = \alpha_2$) and non-symmetric ACs ($\alpha_1 \ne \alpha_2$) is discussed by Li in [9] and [10], respectively. In the previous works, Nguyen and Li examined the effects of gas rarefaction (D and ACs) [18]. Also, the coupled effects of surface roughness and gas rarefaction on the quality factors of MEMS resonators [19] are discussed in a wide range of resonator modes. In addition, the influences of temperature (Nguyen and Li [20]) and relative humidity (Nguyen *et al.* [21]) on the Q-factor of the MEMS resonator under a variety of gas rarefaction (D and ACs (α_1, α_2)) conditions were investigated. However, the effect of surface roughness has not been examined for various types of the gas in gas rarefaction. In this study, the average MMGL equation for the SFD, which is modified with the pressure flow factors (ϕ_{xx}^p, ϕ_{yy}^p), dynamic viscosity (μ) given by Sutherland [22] for various types of the gas, and the database of $Q_P(D,\alpha_1,\alpha_2)$ [17], is used to examine the

effects of surface roughness pattern under various types of the gas and gas rarefaction conditions. The internal structural damping sources (thermoelastic damping (TED) and support loss) are also involved to calculate the total Q-factor of micro-beam resonator. Finally, the roughness pattern effect (H_S, γ) on the Q-factor of MEMS resonators in various types of the gas, gas rarefaction (D, and ACs), and mode of resonator is considered.

2. MATERIALS AND METHODS

In this section, the main energy dissipation sources of the MEMS resonators such as the SFD, TED, and support loss are taken into account under different operation conditions. The main governing equations are: (1) the average MMGL equation (which represents the effect of the surface roughness pattern on the SFD in various types of the gas and gas rarefaction), (2) the transverse motion equation with their boundary conditions of the micro-beam.

2.1. The squeeze film damping (SFD) in MEMS resonators

In a gaseous ambient, the transverse vibration of micro-beam resonators is restricted by an applied load of gas film as structure of micro-beam is squeezed in small gap spacing as depicted in Figure 1. The Poiseuille flow rate occurs as a gas flow is squeezed periodically in a small gap spacing in the normal direction with a substrate. Also, when the transverse movement of micro-beam is influenced by a gas applied load in a thin gap spacing, the resonant frequency and the quality factor of micro-beam resonators can be changed in various type of the gas and gas rarefaction.

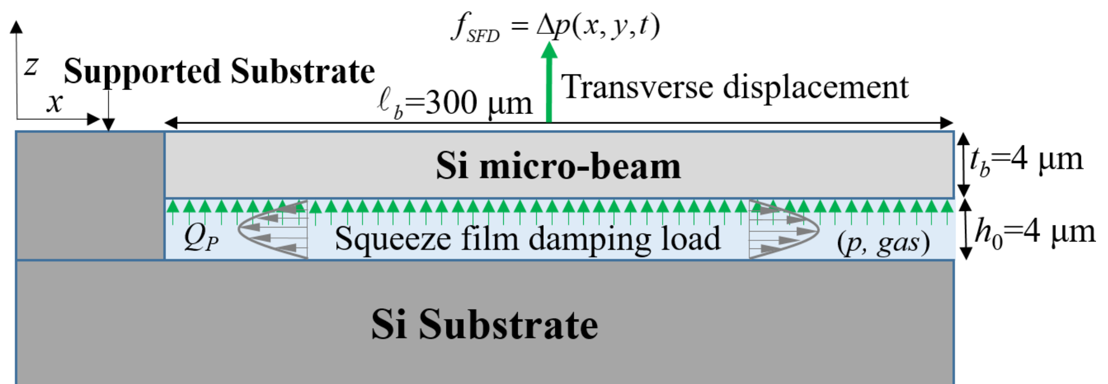

Figure 1. Transverse motion behaviors of micro-beam resonators under the squeeze film damping conditions in various types of the gas.

In an ultra-thin gap spacing, gas film is resisted between two surfaces, z_1 (vibration surface) with the transverse motion in z-direction and z_2 (stationary one) as shown in Figure 2, where the random variables (δ_1 and δ_2) represent a stationary stochastic process distributed with standard deviations of the composite surfaces (σ_1 and σ_2), respectively (Li *et al.* [3]). Under the assumption that the two variables $(\delta_1$ and $\delta_2)$ are uncorrected, the standard deviation (σ) of the roughness combination $(\delta_1 - \delta_2)$ is given simply by $(\sigma_1^2 + \sigma_2^2)^{1/2}$. Thus, at a small gas

pressure and thin gap spacing, the effects of surface roughness and gas rarefaction become important and must be considered in the SFD analysis.

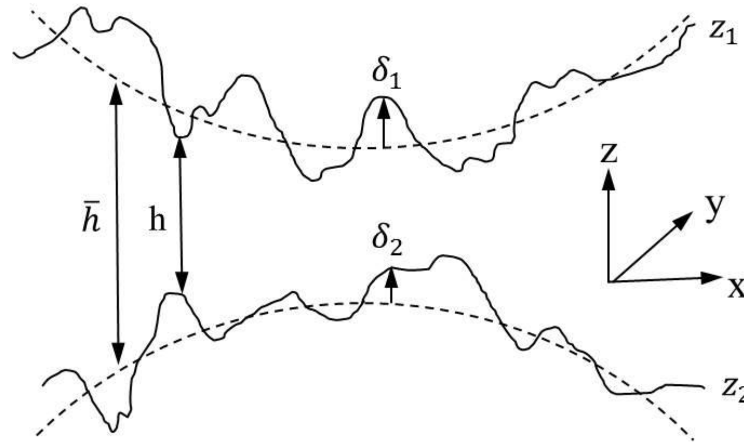

Figure 2. Schematic representation of two roughness surfaces [3].

To consider the effects of roughness pattern in various types of the gas, the pressure flow factors were derived [3] for the average MMGL equation. The complete database of $Q_P(D,\alpha_1,\alpha_2)$ reported by Li [17] is used to modify the average MMGL equation to consider the effect of gas rarefaction. The pressure distribution of the gas flow over the small gap spacing is modeled using the average MMGL equation to consider the influence of the roughness pattern in a wide range of gas rarefaction and various types of the gas as follows:

$$\frac{\partial}{\partial x}\left(\phi_{xx}^{P}\frac{\rho h^3}{12\mu_{eff}}\frac{\partial p}{\partial x}\right)+\frac{\partial}{\partial y}\left(\phi_{yy}^{P}\frac{\rho h^3}{12\mu_{eff}}\frac{\partial p}{\partial y}\right)=\frac{\partial}{\partial t}(\rho h) \tag{1}$$

where p, ρ, and h are the pressure, the density and the gas film spacing, respectively; ϕ_{xx}^{p} and ϕ_{yy}^{p} ($\gamma,\sigma,H_S,D_0,\alpha$) are the pressure flow factors in x and y directions, respectively; H_S ($=h_0/\sigma$) is the film thickness ratio (the roughness height); $\sigma=\left(\sqrt{\sigma_1^2+\sigma_2^2}\right)$ is the roughness height standard deviation of the two surfaces.

The pressure flow factors (ϕ_{xx}^{p} and ϕ_{yy}^{p} ($\gamma,\sigma,H_S,D_0,\alpha$)) are derived as a function of the Peklenik number (γ_i) and the standard deviation (σ_i) of the i-surface, where i = 1,2. They are also functions of film thickness ratio (H_S), and gas rarefaction (inverse Knudsen numbers (D_0) and accommodation coefficients, ACs ($\alpha_1=\alpha_2$)). Thus, the pressure flow factors [3] are represented as below:

$$\phi_{xx}^{p}=1+g\times\left(\frac{\sigma}{\bar{h}}\right)^2\left\{1-\frac{f^2}{g}\frac{1}{\gamma+1}\right\} \tag{2}$$

$$\phi_{yy}^{p} = 1 + g \times \left(\frac{\sigma}{\bar{h}}\right)^{2} \left\{1 - \frac{f^{2}}{g} \frac{\gamma}{\gamma + 1}\right\} \tag{3}$$

$$\phi_{yy}^{p}(\gamma_1, \gamma_2) = \phi_{xx}^{p}\left(\frac{1}{\gamma_1}, \frac{1}{\gamma_2}\right) \tag{4}$$

Though the diagonal flow factors are the same, the off-diagonal flow factors are different.

$$\frac{1}{\gamma + 1} = \left(\frac{\sigma_2}{\sigma}\right)^{2} \frac{1}{\gamma_2 + 1} + \left(\frac{\sigma_1}{\sigma}\right)^{2} \frac{1}{\gamma_1 + 1} \tag{5}$$

$$f(D, \alpha_1, \alpha_2) = 3 + \frac{D \times \partial Q_P / \partial D}{Q_P} \tag{6}$$

$$g(D, \alpha_1, \alpha_2) = 3 + \frac{3D \cdot \partial Q_P / \partial D}{Q_P} + \frac{D^2}{2} \frac{\partial^2 Q_P / \partial D^2}{Q_P} \tag{7}$$

where γ is the Peklenik number. As shown in Figure 3, three types of roughness patterns are represented.

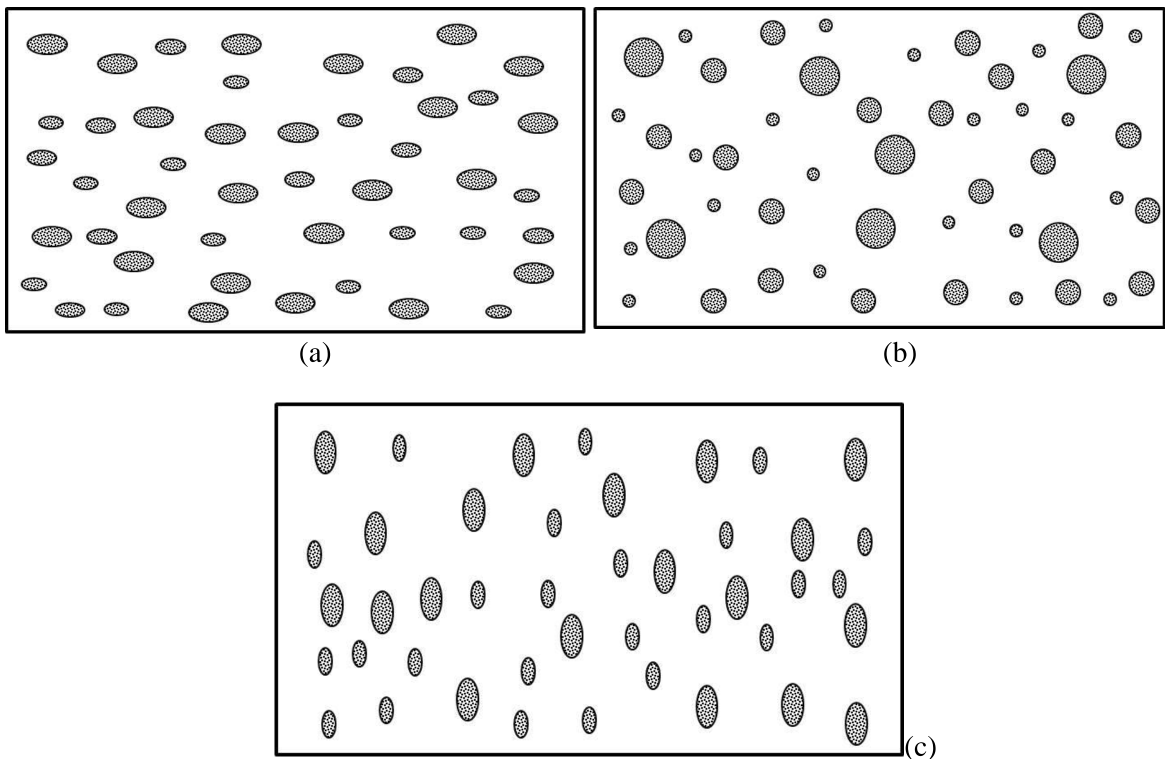

Figure 3. (a) longitudinal type roughness pattern ($\gamma > 1$), (b) isotropic type roughness pattern ($\gamma = 1$), and (c) transverse type roughness pattern ($y < 1$) [8].

The effective viscosity (μ_{eff}) described by Veijola *et al*. [2] is used to consider the gas rarefaction effect as follows:

$$\mu_{eff} = \frac{\mu}{Q_P(D,\alpha_1,\alpha_2)} \tag{8}$$

where μ is the dynamic viscosity of gas, and Q_P is the Poiseuille flow rate corrector, which is the measure of gas flow restriction on the motion of the micro-beams in gas rarefaction.

Sutherland [22] deduced an expression for dynamic viscosity for various types of ideal gas over a wide range of temperatures ($0 < T < 555$ K) as follows:

$$\mu = \mu_0' \frac{T_0' + C}{T + C}\left(\frac{T}{T_0'}\right)^{3/2} \tag{9}$$

where μ_0' is the reference viscosity at the reference temperature (T_0') and C is a Sutherland's constant. Sutherland's constants including C , μ_0', T_0' for various types of ideal gas are provided in Table 1 for analytical calculations of μ .

The database of $\tilde{Q}_P(D,\alpha_1,\alpha_2)$ obtained by solving the linearized Boltzmann equation was used by Li [17] to consider the gas rarefaction effect in a wide range of D ($0.01 \le D_0 \le 100$) and ACs ($0.1 \le \alpha_1, \alpha_2 \le 1.0$) as follows:

$$\tilde{Q}_P(D,\alpha_1,\alpha_2) = \exp\left[\sum_{n=1}^{13} C_n (\ln D)^{13-n}\right] \tag{10}$$

where ACs ($\alpha_1 = \alpha_2$) are the surface accommodation coefficients representing the gas molecules collisions with *i*-solid surface (specular reflection ($\alpha = 1.0$) and diffusive reflection ($\alpha = 0.1$)).

The Poiseuille flow rate corrector of $Q_P(D,\alpha_1,\alpha_2)$ is calculated as the ratio of $\tilde{Q}_P(D,\alpha_1,\alpha_2)$ for rarefied flow to that for continuum flow ($\tilde{Q}_{con}(D) = D/6$), i.e.

$$Q_P(D,\alpha_1,\alpha_2) = \frac{\tilde{Q}_P(D,\alpha_1,\alpha_2)}{\tilde{Q}_{con}(D)} = \frac{6}{D}\tilde{Q}_P(D,\alpha_1,\alpha_2) \tag{11}$$

The first and second derivations of gas rarefaction coefficients ($\tilde{Q}_P$) with respect to (D,α_1,α_2) are given by the following expressions:

$$\frac{\partial Q_p}{\partial D} = -\frac{6}{D^2}\tilde{Q}_p + \frac{6}{D}\frac{\partial \tilde{Q}_p}{\partial D} \tag{12a}$$

$$\frac{\partial \tilde{Q}_p}{\partial D} = \frac{1}{D}\tilde{Q}_p\left[\sum_{n=1}^{12}(13-n)C_n(\ln D)^{12-n}\right] \tag{12b}$$

$$\frac{\partial^2 Q_p}{\partial D^2} = \frac{12}{D^3}\tilde{Q}_p - \frac{12}{D^2}\frac{\partial \tilde{Q}_p}{\partial D} + \frac{6}{D}\frac{\partial^2 \tilde{Q}_p}{\partial D^2} \tag{13a}$$

$$\frac{\partial^2 \tilde{Q}_p}{\partial D^2} = \left[-\frac{1}{D}\frac{\partial \tilde{Q}_p}{\partial D}\right] + \left[\frac{1}{\tilde{Q}_p}\left(\frac{\partial \tilde{Q}_p}{\partial D}\right)^2\right] + \frac{1}{D^2}\tilde{Q}_p\left[\sum_{n=1}^{11}(13-n)(12-n)C_n(\ln D)^{11-n}\right] \tag{13b}$$

The inverse Knudsen number (D), which is an important gas rarefaction indicator, is calculated by

$$D = \frac{\sqrt{\pi}}{2K_n} = \frac{\sqrt{\pi}h}{2\lambda} \tag{14}$$

where K_n $(=\lambda_p / h_0)$ is the Knudsen number representing the gas rarefaction.

The mean free path of gas (λ) can be evaluated in the physical model [23] as below:

$$\lambda = \frac{k_B T}{\sqrt{2}\pi \cdot d^2 p} \tag{15}$$

where $k_B = 1.380658 \times 10^{-23}$ (J/K) is the Boltzmann constant, and d is the diameter of the cross section of particles given by Kennard [24].

An alternative method to calculate the mean free path of the gas (λ) as a function of pressure (p) at a constant temperature [16] is given by

$$\lambda = \lambda_0 \frac{p_0}{p} \tag{16}$$

where λ_0 is the reference mean free path of the gas at reference pressure (p_0 = 101325 Pa) and 300 K for different types of the gas as shown in Table 1.

Table 1. The reference parameters for dynamic viscosities (μ) and mean free paths (λ) for various types of ideal gas.

Gas	C (K) Sutherland [22]	T_0' (K) Sutherland [22]	μ_0' (μPa.s) Sutherland [22]	d (Å) Kennard [24]	λ_0 (nm) (Eq.(15)) at 101325 Pa & 300 K	μ (μPa.s) (Eq.(9)) at 300 K
Air	120	291.15	18.27	3.72	66.487	18.71
Helium (He)	79.4	273	19	2.18	193.6	20.33
Oxygen (O_2)	127	292.25	20.18	3.61	70.601	20.61
Carbon dioxide (CO_2)	240	293.15	14.8	4.59	43.672	15.13
Hydrogen (H_2)	72	293.85	8.76	2.74	122.55	8.887
Nitrogen (N_2)	111	300.55	17.81	3.75	65.428	17.79
Argon (Ar)	133	298	22.6	3.64	69.442	22.72

2.2. Transverse vibration of micro-beam resonators

In a small gap spacing, the vibration of the micro-beam is resisted by a gas fluid force. We consider the transverse vibrations of micro-beam affected by a net external force, $f_{ext} = \Delta p(x, y, t)$ per unit area on the boundary of the micro-beams (Figure 1). Under the small

variation of beam deflection, the linear equation for the transverse vibration of the microplate [25] is given by

$$D_b\left(\frac{\partial^4 w}{\partial x^4}+2\frac{\partial^4 w}{\partial x^2\partial y^2}+\frac{\partial^4 w}{\partial y^4}\right)+\rho_S t_b\frac{\partial^2 w}{\partial t^2}=-\Delta p(x,y,t) \tag{17}$$

where $w(x, y, t)$ is the small transverse deflection of the micro-beams as a function of positions x, y, and time t; $D_b\,(=Et_b^3/12(1-\nu^2))$ is the rigidity of the beam structure; E is the Young's modulus of the beam; ρ_S is the density of the beam; t_b is the beam thickness, and ν is the Poisson's ratio.

The boundary conditions of the micro-beams are given by clamped edge at $x=0$

$$w(x,y,t)=0;\ \frac{\partial w(x,y,t)}{\partial x}=0 \tag{18}$$

and free edges at $y=0$, $y=w_b$, and $x=\ell_b$

$$\frac{\partial^2 w(x,y,t)}{\partial x^2}=\frac{\partial^3 w(x,y,t)}{\partial x^3}=0 \tag{19}$$

$$\frac{\partial^2 w(x,y,t)}{\partial y^2}=\frac{\partial^3 w(x,y,t)}{\partial y^3}=0 \tag{20}$$

For the SFD, the eigenvalues of the average MMGL equation (Eq.(1)), the transverse motion equation (Eq.(17)), and boundary conditions of micro-beam resonators (Eqs. (18 - 20)) are simultaneously solved by the Finite Element Method (FEM) [26]. Thus, the eigenvalues ($\bar{\lambda}=\delta+i\omega$) including the damping factor ($\delta=\mathrm{Re}(\bar{\lambda})$) and the natural frequencies ($\omega=\mathrm{Im}(\bar{\lambda})$) are obtained from solving these equations [18].

2.3. Quality factor

For MEMS resonators, the Q-factor is the ratio between the resonant frequency (ω_0) and its bandwidth ($\Delta\omega$) of the resonant spectrum as given by

$$Q=\frac{2\pi W_0}{\Delta W}=\frac{\omega_0}{\Delta\omega} \tag{21}$$

In the eigenvalue problem, an equivalent definition (Nguyen and Li [18]) becomes more accurate to calculate the Q-factor of MEMS resonators as below:

$$Q=\frac{\omega_0}{2\delta}=\left|\frac{\mathrm{Im}(\bar{\lambda})}{2\,\mathrm{Re}(\bar{\lambda})}\right| \tag{22}$$

from the eigenvalues for *n*-transverse modes of MEMS resonator ($\bar{\lambda}_n=\delta_n+i\omega_n$), the Q-factor for the SFD problem (Q_{SFD}) can be evaluated for *n*-modes of MEMS resonators.

In micro-beam resonators, the total Q-factor (Q_T) can be calculated by summing the contributions of the Q-factors from dominant damping sources such as SFD (Q_{SFD}), TED (Q_{TED}) and support loss (Q_{sup}) [18, 19] as follows:

$$\frac{1}{Q_T}=\frac{1}{Q_{SFD}}+\frac{1}{Q_{TED}}+\frac{1}{Q_{\sup}}=\frac{1}{Q_{SFD}}+\frac{1}{Q_{TA}} \tag{23}$$

where Q_{SFD} can be obtained by solving the complex eigenvalue ($\bar{\lambda}$) in the eigenvalue problem of the linear equations (Eq.(1) and Eq. (17)) with their appropriate boundary conditions (Eqs. (18 - 20)). $1/Q_{TA}$ $(=1/Q_{TED}+1/Q_{\sup})$ is the internal structural damping of the micro-beam resonators. Q_{TED} and $Q_{\sup}$ can be obtained from Table 3 and Table 4, respectively, as described by Nguyen and Li [18, 19].

3. RESULTS AND DISCUSSION

In thin clearance, the effect of surface roughness must be considered under gas ambient conditions. For the SFD problem, pressure flow factors ((ϕ_{xx}^P) and (ϕ_{yy}^P)) (Eqs.(2)-(7)) are correctors for surface roughness. The effective viscosity (μ_{eff}) is defined as the ratio between dynamic viscosity (μ) by Sutherland [22] (considering various types of ambient gas) and Poiseuille flow rate ($Q_P(D,\alpha_1,\alpha_2)$) by Li [17] (Eqs.(10-13)) (the correctors for the gas rarefaction). In addition, the database of $Q_P(D,\alpha_1,\alpha_2)$ reported by Li [17] is applicable for use in arbitrary D_0 and ACs. Basic operating conditions are listed in Table 2. The average MMGL equation (Eq. (1)) for the SFD problem is modified by effective viscosity (μ_{eff}). Finally, the effect of surface roughness pattern (H_S , γ) on the Q-factors of micro-beam resonator in various types of the gas, gas rarefaction (D_0 and ACs), and resonator mode is considered.

Table 2. Basic operating conditions of micro-beam resonators.

Parameter	Description	Values
ℓ_b	length of micro-beam	300 μm
w_b	width of micro-beam	22 μm
t_b	thickness of micro-beam	4 μm
E	Young modulus of poly-silicon	160×10^9 Pa
ρ_S	density of poly-silicon	2330 Kg/m^3
v	Poisson's ratio of poly-silicon	0.22
α_S	thermal expansion coefficient of poly-silicon	2.6×10^{-6} 1/K
κ	thermal conductivity of poly-silicon	90 W/(m K)
C_p	specific heat capacity of poly-silicon	700 J/(Kg K)
T_0	temperature	300 K
μ	dynamic viscosity	1.871×10^{-5} Pa s
h_0	gas film thickness	4 μm
p_0	reference pressure of air	101325 Pa
λ_{p0}	reference molecular mean free path of air at p_0	66.5 nm
p_{basic}	basic ambient pressure for air	190.0786 Pa
D	inverse Knudsen number	0.1
ACs	Surface accommodation coefficients (α_i)	1.0
H_S	Film thickness ratio of surface roughness height	3
γ	Longitudinal Peklenik number of roughness pattern	9

3.1. Pressure flow factors, (ϕ_{xx}^{P})

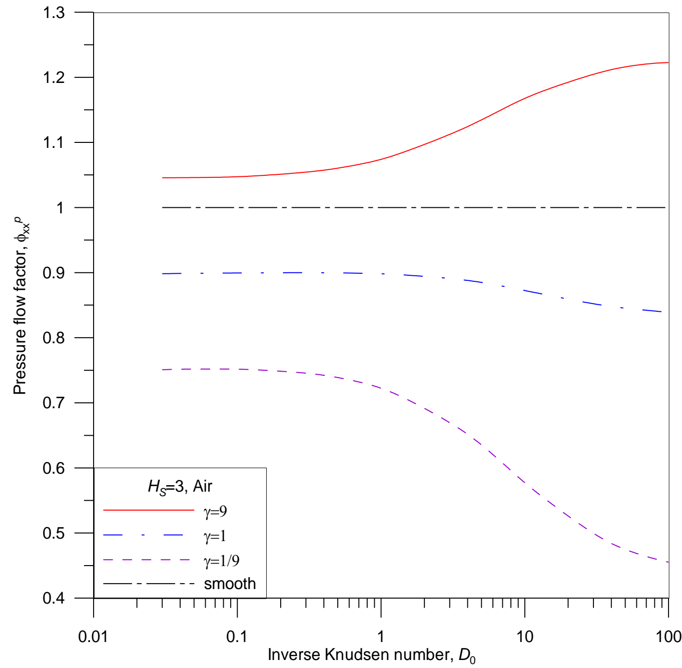

Figure 4. Pressure flow factor (ϕ_{xx}^{p}) plotted with inverse Knudsen number (D_0) for different Peklenik numbers (γ) in air.

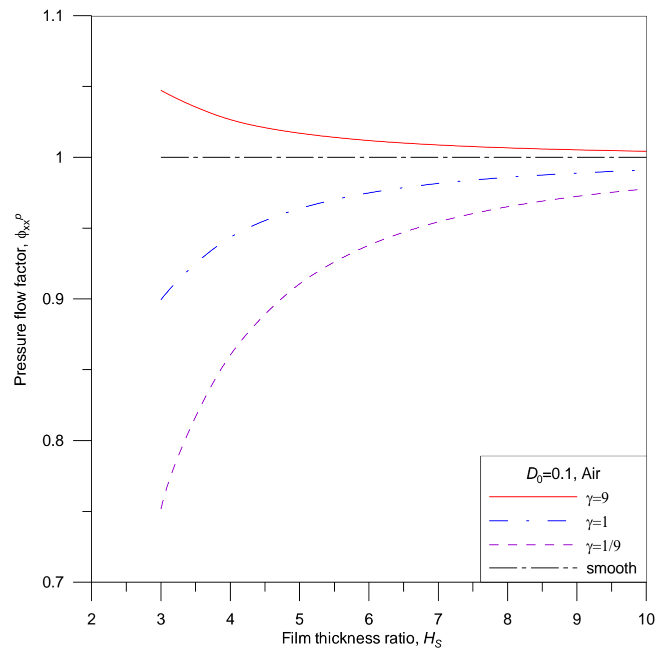

Figure 5. Pressure flow factor (ϕ_{xx}^{p}) plotted with film thickness ratio (H_S) for different Peklenik numbers (γ).

In Figure 4, pressure flow factor (ϕ_{xx}^{P}) increases as D_0 increases (gas rarefaction decreases and gas flow becomes more restricted) for the longitudinal type roughness pattern ($\gamma = 9$). Meanwhile, ϕ_{xx}^{P} decreases and moves further away for the case of smooth surface (ϕ_{xx}^{P}=1) as D_0 increases and γ decreases for the isotropic type roughness ($\gamma = 1$) and the transverse type roughness ($\gamma = 1/9$). Therefore, it is possible for the present model to consider the surface roughness pattern effects (H_S, γ) on the Q-factors of MEMS resonators in a wide range of gas rarefaction (D and ACs(α_1,α_2)).

In Figure 5, the pressure flow factor (ϕ_{xx}^{P}) is plotted as a function of the film thickness ratio (H_S) for different Peklenik numbers (γ). The results show that ϕ_{xx}^{P} gradually decreases to nearly 1 (smooth case) when the film thickness ratio (H_S) increases for the longitudinal surface roughness pattern (γ = 9). The surface roughness pattern effect is reduced as H_S increases or surface roughness height decreases. In the meantime, ϕ_{xx}^{P} increases to nearly 1 as H_S increases from the isotropic type surface roughness (γ =1) to the transverse type surface roughness (γ = 1/9) ($\phi_{xx}^{P}(\gamma=1) > \phi_{xx}^{P}(\ )$). At lower H_S, ϕ_{xx}^{P} changes with γ more considerably because the gas flow in thin gap spacing becomes more restricted and the surface roughness pattern effect becomes more strongly.

3.2. Effective viscosity, μ_{eff} $(= \mu / Q_P)$

The reference parameters used to calculate the dynamic viscosity (μ) and the mean free path (λ) for various types of the gas are listed in Table 1. In Figure 6, the results show that λ decreases as p increases (Figure 6(a)), and then Q_p decreases as p increases for various types of the gas (Figure 6(b)). In Figure 6(c), μ_{eff} (=μ/Q_P) increases as pressure (p) increases for various types of the gas. Different types of the gas exhibit different behaviors of μ_{eff} over a wide pressure range because they have different values of μ (Table 1) and Q_p (Figure 6(b)) under various pressure conditions. Furthermore, μ_{eff} for He and H_2 is less than those for the other gases (Ar, O_2, Air, N_2, and CO_2) in a wide range of pressure conditions. The obtained results can be applied to discuss the effects of surface roughness pattern (H_S, γ) to improve the Q-factors of MEMS resonators under various types of the gas and gas rarefaction conditions.

3.3. Resonant frequency (ω), damping factor (δ), and quality factor (Q_{SFD})

It can be seen from Figure 7(a) that ω_n increases and then decreases with increasing pressure because the spring force of the gas film increases more than the damping force as the pressure increases [8]. In Figure 7(b), the damping factor (δ) of the SFD increases and reaches its maximum value as the ambient pressure increases. Thus, Q_{SFD} reduces and reaches its minimum value as the pressure increases (Figure 7(c)) because the gas flow becomes more restricted when the pressure is increased or higher SFD is produced. To consider the surface

roughness effect, three types of surface roughness pattern (γ =9, 1, 1/9) are used. The results show that ω_n varies significantly as γ increases (Figure 7(a)). Moreover, ω_n varies with γ more considerably in the case of air than in the case of H_2 (because the effective viscosity (μ_{eff}) of air is greater than that of H_2 as seen in Figure 6(c)).

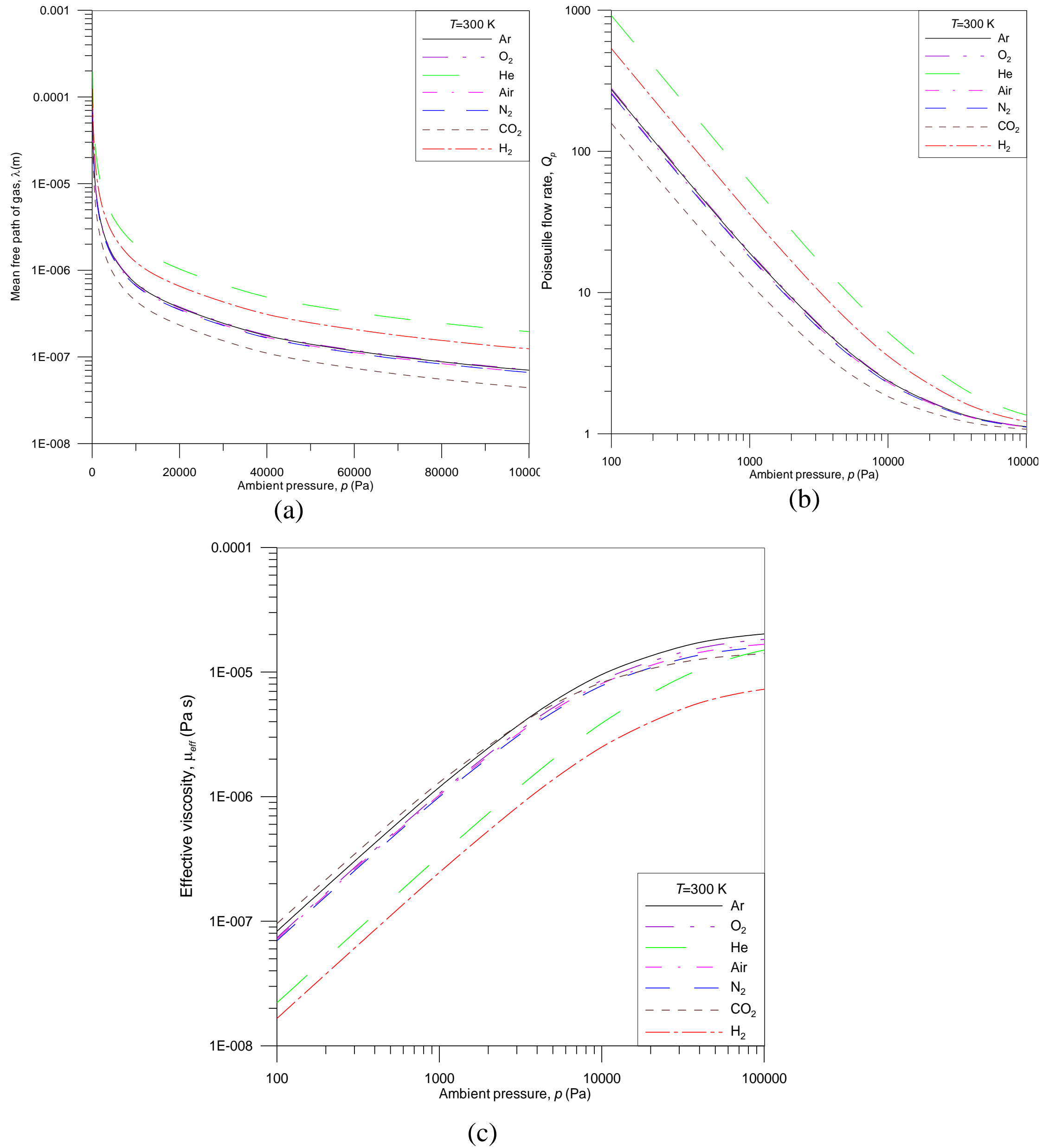

Figure 6. (a) Mean free path of gas (λ), (b) Poiseuille flow rate (Q_p), and (c) effective viscosity (μ_{eff}) plotted with ambient pressure (p) for different types of the gas.

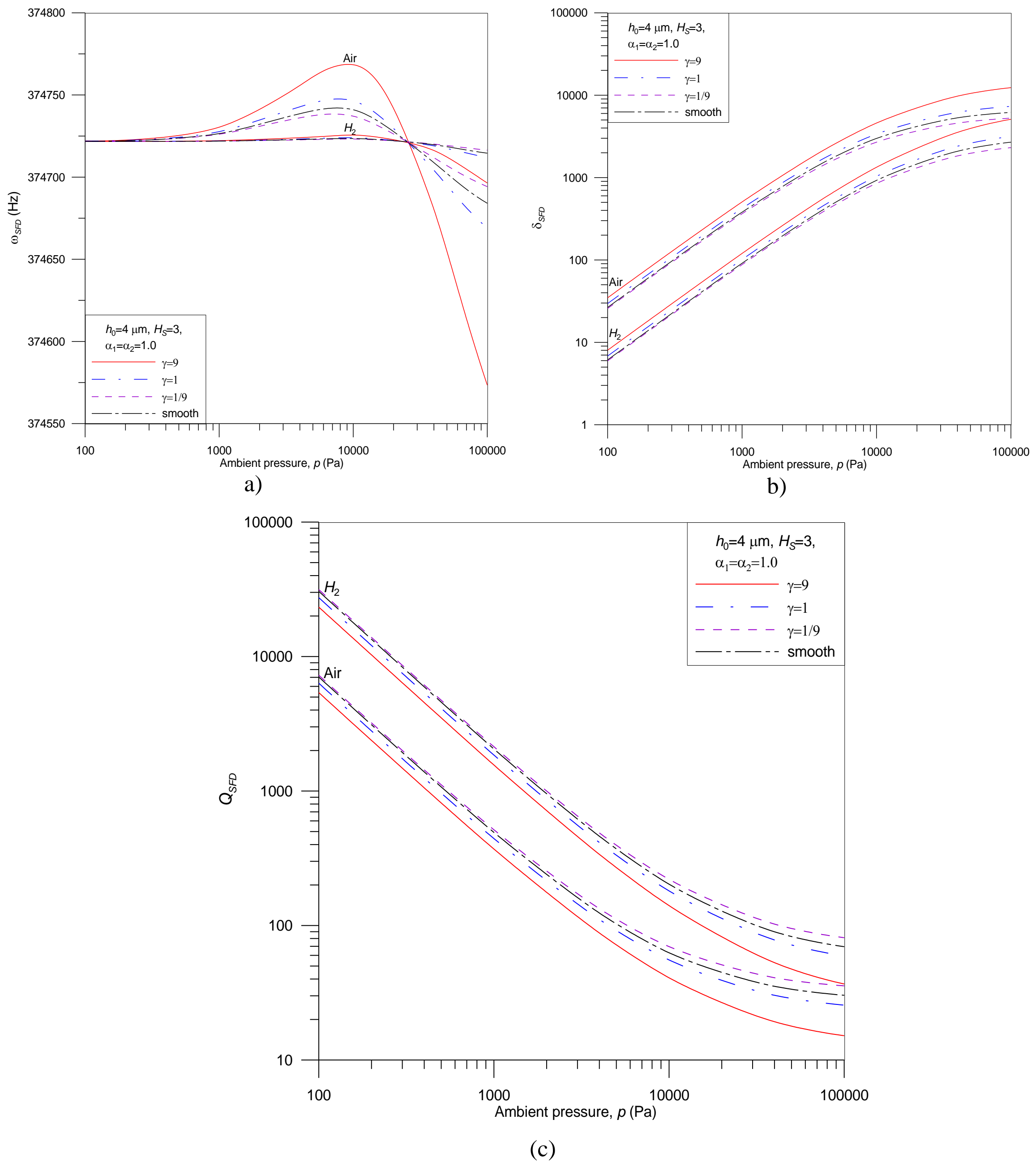

Figure 7. (a) Resonant frequency ($\omega_n = 2\pi f_n$), (b) Damping factor (δ), and (c) Q-factor for the SFD ($Q_{SFD} = \omega_n / (2 \cdot \delta)$) plotted with pressure for different Peklenik numbers (γ) and different types of the gas (Air and H_2).

Also, δ increases as γ increases (Figure 7(b)) and thus, Q_{SFD} decreases with increasing γ, i.e. Q_{SFD} (γ =1/9) > Q_{SFD} (smooth) > Q_{SFD} (γ =1) > Q_{SFD} (γ =9) (Figure 7(c)). Apart from that, the effect of surface roughness pattern (γ) on Q_{SFD} becomes more considerably as the

ambient pressure (p) and the effective viscosity (μ_{eff}) of gases increase. Thus, the surface roughness pattern effect (γ) on Q-factor of SFD (Q_{SFD}) is enhanced and becomes more significantly in lower gas rarefaction (higher pressure) and higher effective viscosity (μ_{eff}) of gases.

3.3. Quality factors, Q_{SFD} and Q_T

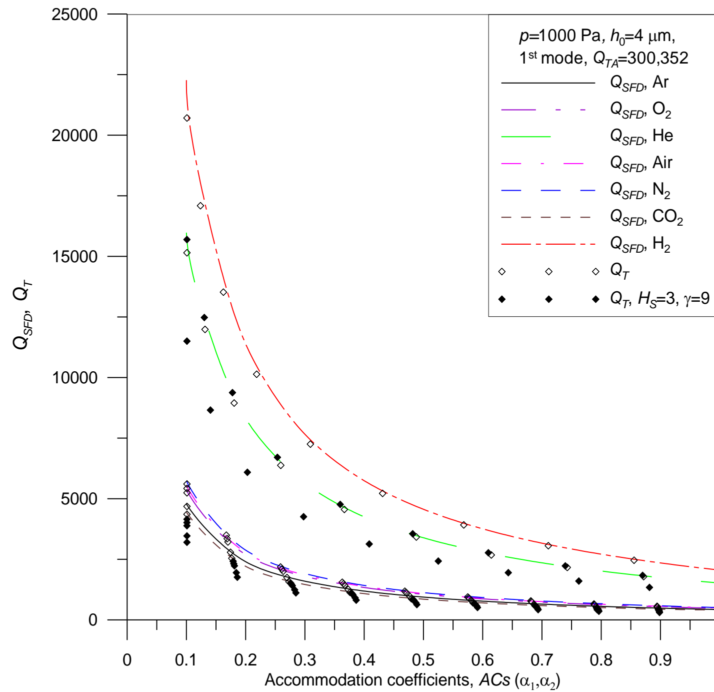

Figure 8. Q-factor of SFD (Q_{SFD}) and total Q-factor (Q_T) plotted with the ACs α ($\alpha_1 = \alpha_2$) for different types of the gas and the longitudinal roughness pattern ($\gamma = 9$ and $H_S = 3$).

In Figure 8, Q_{SFD} and total Q-factor (Q_T) are plotted for different types of the gas in a wide range of ACs ($\alpha_1 = \alpha_2$) under the smooth and roughness (H_S = 3, γ = 9) conditions. Q_{SFD} and Q_T increase simultaneously as ACs ($\alpha_1 = \alpha_2$) decrease because the gas film is less restricted and lower SFD is produced as gas rarefaction increases (ACs decrease). Also, the values of Q_{SFD} almost approach those of Q_T in the smooth case for various types of the gas in a wide range of ACs ($\alpha_1 = \alpha_2$) because the SFD is dominant. In addition, the gas flow is squeezed and then enhanced for the longitudinal type of roughness pattern ($H_S = 3, \gamma = 9$). Then, the Q_T ($H_S = 3, \gamma = 9$) is less than Q_{SFD} and Q_T (smooth case) for different types of the gas. Thus, the surface roughness patterns (H_S and γ) clearly affect Q_{SFD}, Q_T for different types of the gas in a wide range of ACs ($\alpha_1 = \alpha_2$).

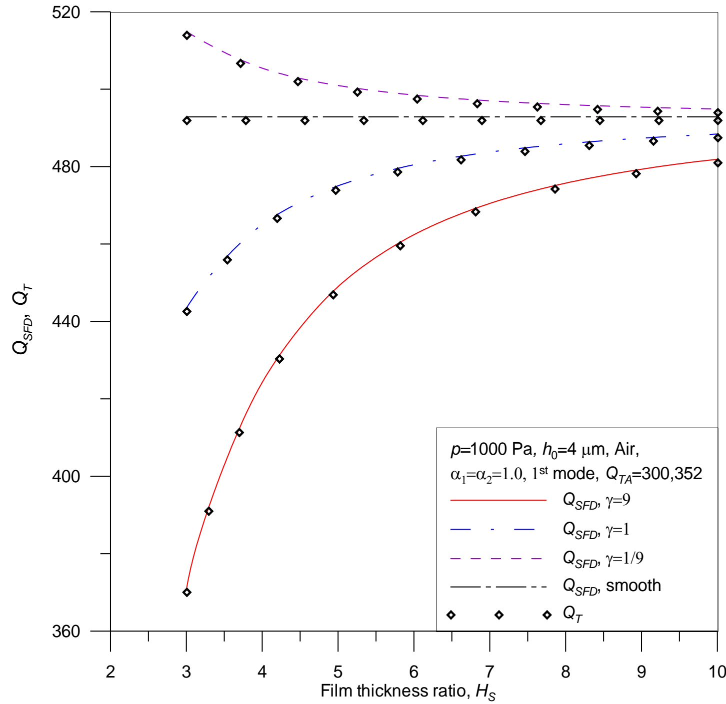

Figure 9. Q_{SFD} and Q_T versus film thickness ratios (H_S) for different Peklenik numbers (γ).

In Figure 9, Q_{SFD} and Q_T are plotted as the functions of film thickness ratio (H_S) for different Peklenik numbers (γ) in the 1st mode of resonator. The results show that Q_{SFD} increases as surface roughness pattern varies from the longitudinal type (γ=9) to isotropic type (γ=1) and transverse type (γ=1/9) because of the change in the pressure flow factor (ϕ_{xx}^P) under various γ and H_S conditions (Figure 5). In addition, the values of Q_{SFD} almost approach those of Q_T in a wide range of surface roughness patterns (H_S and γ) in the 1st mode of resonator because the SFD is dominant. Also, Q_{SFD} and Q_T tend to approach the smooth surface as H_S increases for various surface roughness patterns (γ). The obtained results can be used to discuss changes in the ratio of $Q_T / (Q_T)_{smooth}$ for different surface roughness patterns (H_S, γ) in various types of the gas, gas rarefaction and mode of resonator.

In Figure 10, the ratio of $Q_T /(Q_T)_{smooth}$ is plotted as a function of the film thickness ratio (H_S) at different Peklenik numbers (γ) with various types of the gas for different resonator modes in high gas rarefaction (p = 1000 Pa). It can be seen from Figure 10(a) that the ratio of $Q_T /(Q_T)_{smooth}$ varies with the effect of surface roughness pattern (H_S and γ) in a way similar to that of Q_{SFD} and Q_T in Figure 9. In addition, the variation of the $Q_T /(Q_T)_{smooth}$ ratio with respect to H_S and γ is almost unchanged for various types of the gas in the 1st resonator mode (SFD is dominant), while the $Q_T /(Q_T)_{smooth}$ ratio tends to approach the smooth case more quickly for various types of the gas as the mode of resonator increases (see Figures 10(b-d)). That is because the internal structural damping (TA) increases (an increase of $(Q_{TA})^{-1}$ in Eq.

(23)) and the external SFD decreases (a decrease of $(Q_{SFD})^{-1}$ in Eq. (23)) as the resonator mode increases.

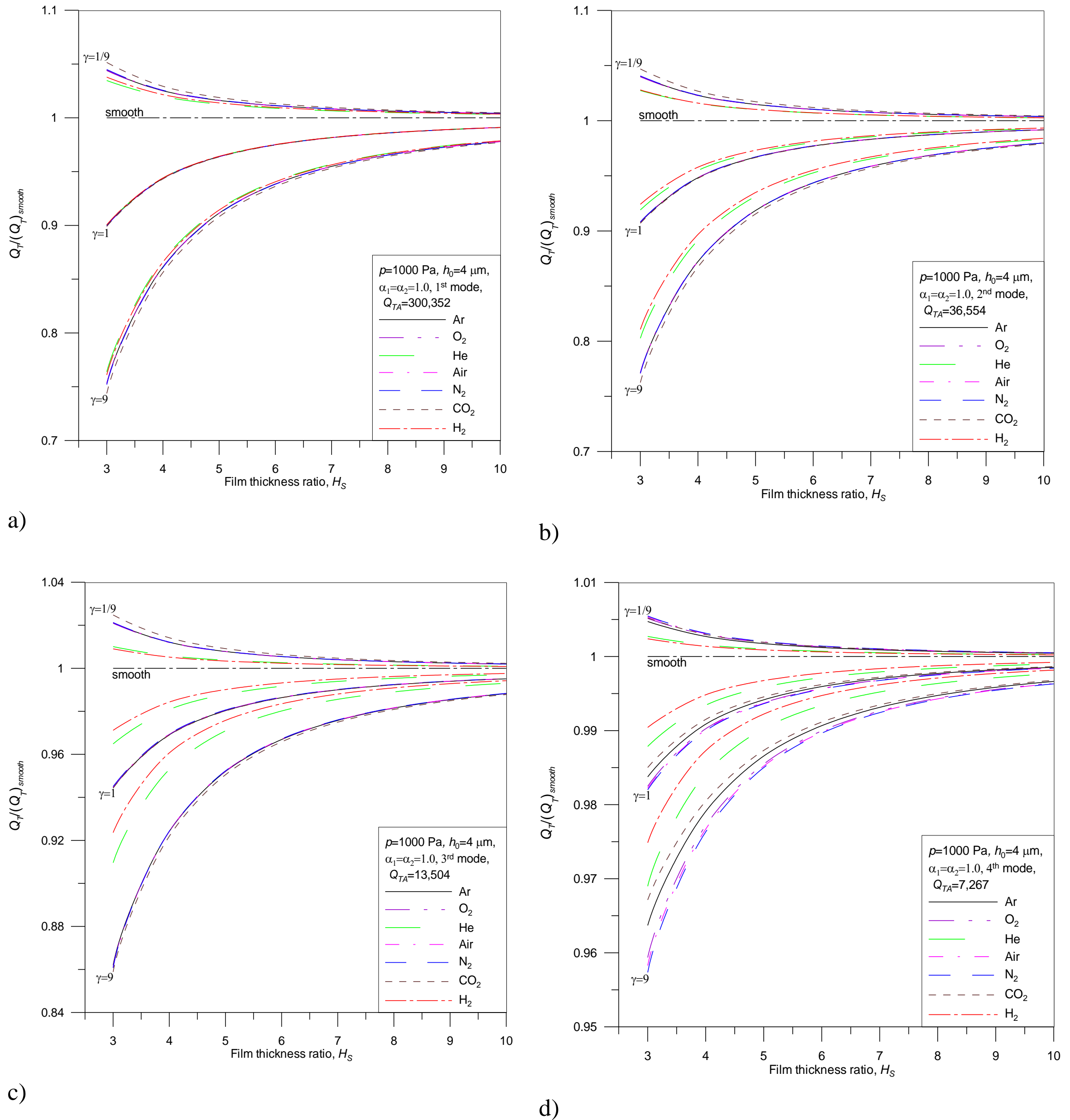

Figure 10. Ratio of $Q_T/(Q_T)_{smooth}$ plotted with film thickness ratio (H_S) at different Peklenik numbers (γ) with various types of the gas in gas rarefaction (p = 1000 Pa) for (a) 1st mode, (b) 2nd mode, (c) 3rd mode, and (d) 4th mode of resonator.

Also, the $Q_T/(Q_T)_{smooth}$ ratio varies with surface roughness patterns (H_S and γ) more considerably and tends to approach the smooth case more quickly with gases of higher effective

viscosity (such as Ar, O_2, Air, N_2, CO_2) compared to lower effective viscosity gases (He and H_2) in a higher mode of resonator and gas rarefaction (p = 1000 Pa) (see Figures 10(b-d)). Thus, the effect of surface roughness pattern (H_S and γ) on $Q_T/(Q_T)_{smooth}$ decreases more significantly as the effective viscosity of gases decreases in higher mode of resonator and higher gas rarefaction.

4. CONCLUSIONS

The average MMGL equation is modified with the pressure flow factors, (ϕ_{xx}^P, ϕ_{yy}^P), the database of $Q_P(D,\alpha_1,\alpha_2)$ provided by Li [17], and the dynamic viscosity determined by Sutherland [22] to consider the effect of surface roughness pattern for various types of the gas and gas rarefaction. The Q-factors of the external SFD and the internal structural damping (TA) are taken into account to calculate the total Q-factor. Thus, the Q-factor due to the SFD (Q_{SFD}) and the total Q-factor (Q_T) are studied under the effect of surface roughness pattern (H_S and γ) for various types of the gas, gas rarefaction (pressure and ACs), and mode of the resonator. Some important results are summarized below:

a) The effect of surface roughness (H_S,γ) on ω_n, δ_{SFD}, and Q_{SFD} become more significant at higher effective viscosity (μ_{eff}) of the gas and lower gas rarefaction (higher ambient pressure and ACs) due to the increased SFD in the 1st mode of the resonator.

b) The effect of surface roughness pattern (H_S,γ) on the $Q_T/(Q_T)_{smooth}$ratio is almost insensitive to various types of the gas in the 1st mode of the resonator and higher gas rarefaction. Meanwhile, this effect is significantly reduced as the effective viscosity of the gas decreases in the higher mode of the resonator and higher gas rarefaction

Acknowledgements. This research was supported by the Institute for Computational Science and Technology (ICST), Contract Number: 08/2019/HĐ-KHCNTT in October 24th, 2019 and series number: 082019-311. This research was supported by the annual projects of The Research Laboratories of Saigon High Tech Park in 2020 according to decision No. 390 /QĐ-KCNC in December 30, 2019 of Management Board of Saigon High Tech Park (Project number 1).

CRediT authorship contribution statement. Author 1: Investigation, Funding acquisition. Author 2: Investigation. Author 3: Formal analysis, Investigation. Author 4: Formal analysis, Investigation. Author 5: Formal analysis, Investigation. Author 6: Formal analysis, Methodology, Supervision.

Declaration of competing interest. The authors declare that they have no known competing financial interests or personal relationships that could have appeared to influence the work reported in this paper.

REFERENCES

1. Zhang W. M., Hu K. M., Peng Z. K.and Meng G. - Tunable Micro- and Nanomechanical Resonators, Sensors. **15** (10) (2015) 26478-26566.
2. Veijola T., Kuisma H., Lahdenperä J. and Ryhänen T. - Equivalentcircuit model of the squeezed gas film in a silicon accelerometer, Sensor. Actuat. A-Phys. **48** (3) (1995) 239-248.

3. Li W. L., Weng C. l.and Hwang C. C. - Effects of roughness orientations on thin film lubrication of a magnetic recording system, J. Phys D: Appl. Phys. **28** (1995) 1011-1021.
4. Hamrock B. J. - Fundamentals of Fluid Film Lubrication, McGraw-Hill, New York, 1994.
5. Fukui S. and Kaneko R. - Analysis of Ultra-Thin Gas Film Lubrication Based on Linearized Boltzmann Equation: First Report - Derivation of a Generalized Lubrication Equation Including Thermal Creep Flow, J. Tribol-T. ASME. **110** (2) (1988) 253-261.
6. Mitsuya Y. - A Simulation Method for Hydrodynamic Lubrication of Surfaces with Two-Dimensional Isotropic or Anisotropic Roughness Using Mixed Average Film Thickness, Bulletin of J. SME. **27** (231) (1984) 2036-2044.
7. Li W. L.and Weng C. I. - Modified average Reynolds equation for ultra-thin film gas lubrication considering roughness orientations at arbitrary Knudsen numbers, Wear. **209** (1-2) (1997) 292-300.
8. Li W. L. - Analytical modelling of ultra-thin gas squeeze film, Nanotechnology. **10** (4) (1999) 440-446.
9. Li W. L. - Modeling of Head/Disk Interface-An Average Flow Model, Tribol. Lett. **17** (3) (2004) 669-676.
10. Li W. L. - Squeeze film effects on dynamic performance of MEMS μ-mirrors-consideration of gas rarefaction and surface roughness, Microsyst. Technol. **14** (3) (2008) 315-324.
11. Zhang W. M., Meng G., Peng Z. K. and Chen D. - Coupled Nonlinear Effects of Random Surface Roughness and Rarefaction on Slip Flow in Ultra-Thin Film Gas Bearing Lubrication, J. Tribol-T. ASME. **134** (2012a) 024502.
12. Patir N. and Cheng H. S. - An Average Flow Model for Determining Effects of Three-Dimensional Roughness on Partial Hydrodynamic Lubrication, J. Tribol-T. ASME. **100** (1) (1978) 12-17.
13. Bhushan B. and To□nder K. - Roughness-Induced Shear- and Squeeze-Film Effects in Magnetic Recording-Part I: Analysis, J. Tribol-T. ASME. **111** (1989a) 220-227.
14. Bhushan B. and To□nder K. - Roughness-Induced Shear- and Squeeze-Film Effects in Magnetic Recording-Part II: Applications, J. Tribol-T. ASME. **111** (1989b) 228-237.
15. Chang K. M., Lee S. C. and Li S. H. - Squeeze film damping effect on a MEMS torsion mirror, J. Micromech. Microeng. **12** (2002) 556-561.
16. Pandey A. K. and Pratap R. - Coupled nonlinear effects of surface roughness and rarefaction on squeeze film damping in MEMS structures, J. Micromech. Microeng. **14** (2004) 1430-1437.
17. Li W. L. - A Database for Interpolation of Poiseuille Flow Rate for Arbitrary Knudsen Number Lubrication Problems, J. Chin. Inst. Eng. **26** (4) (2003) 455-466.
18. Nguyen C. C. and Li W. L. - Effect of gas rarefaction on the quality factors of micro-beam resonators, Microsyst. Technol. **23** (2016a) 3185-3199.
19. Nguyen C. C. and Li W. L. - Effects of surface roughness and gas rarefaction on the quality factor of micro-beam resonators, Microsyst. Technol. **23** (2016b) 3489-3504.
20. Nguyen C. C. and Li W. L. - Influences of temperature on the quality factors of micro-beam resonators in gas rarefaction, Sens. Actuators. A. Phys. **261** (2017) 151-165.

21. Nguyen C. C., Ngo V. K. T., Le H. Q., and Li W. L. - Influences of relative humidity on the quality factors of MEMS beam resonators in gas rarefaction, Microsyst. Technol. **25** (2018) 2767-2782.
22. Sutherland W. - The viscosity of gases and molecular force, Philos. Mag. Series. **5** (36) (1893) 507-531.
23. Chapman S. and Cowling T. G. - The Mathematical Theory of Non-uniform Gases: An Account of the Kinetic Theory of Viscosity, Thermal Conduction and Diffusion in Gases, Cambridge University Press, Cambridge, England, 1970, pp. 86-96.
24. Kennard E. H. - Kinetic Theory of Gases with an Introduction to Statistical Mechanics, McGraw-Hill, New York and London, 1938, pp. 149.
25. Leissa A.W. - Vibration of Plates, NASA, Washington DC, 1969, pp. 1-6.
26. Reddy J. N. - An introduction to the finite element method, McGraw-Hill, New York, 1993.